Drug Design, Development and Therapy

Dovepress
Taylor & Francis Group

Open Access Full Text Article

ORIGINAL RESEARCH

Tomatidine Alleviates Intervertebral Disc Degeneration by Activating the Nrf2/HO-1/GPX4 Signaling Pathway

Ze Li[1,2,*], Pu Cheng[1,2,*], Huifeng Xi[1,2,*], Ting Jiang[1,2], Xiaohang Zheng[1,2], Jianxin Qiu[1,2], Yuhang Gong[1,2], Xinyu Wu[1,2], Shuang Mi[1,2], Yuzhen Hong[3], Zhenghua Hong[1,2], Weiwei Zhou[1,2]

[1]Department of Orthopaedics, Taizhou Hospital Affiliated to Wenzhou Medical University, Linhai, Zhejiang Province, People's Republic of China; [2]Bone Development and Metabolism Research Center of Taizhou Hospital, Linhai, Zhejiang Province, People's Republic of China; [3]School of Medicine, Wuhan University of Science and Technology, Wuhan, Hubei Province, 430065, People's Republic of China

*These authors contributed equally to this work

Correspondence: Weiwei Zhou; Zhenghua Hong, Department of Orthopaedics, Taizhou Hospital Affiliated to Wenzhou Medical University, Taizhou Linhai City, Zhejiang Province, People's Republic of China, Email zww@enzemed.com; 0001hzh@163.com

Purpose: Intervertebral disc degeneration (IDD) is a leading cause of low back pain, and developing new molecular drugs and targets for IDD is a new direction for future treatment strategies. The aim of this study is to investigate the effects and mechanisms of tomatidine in ameliorating lumbar IDD.

Methods: Nucleus pulposus cells (NPCs) exposed to lipopolysaccharides were used as an in vitro model to investigate changes in the expression of extracellular matrix components and associated signaling pathway molecules. A lumbar instability model was used to simulate IDD. Tomatidine (Td) was then administered intraperitoneally, and its effects were evaluated through histopathological analysis.

Results: In vitro, Td significantly promoted ECM anabolism, inhibited ECM catabolism, and reduced oxidative stress and ferroptosis in LPS-stimulated NPCs. When Nrf2 expression was inhibited, oxidative stress and ferroptosis were exacerbated, and the protective effects of Td on NPCs were lost, suggesting the Nrf2/HO-1/GPX4 axis is critical for the therapeutic effects of Td. In vivo, histopathological analysis demonstrated that Td ameliorated IDD in a murine model.

Conclusion: Td alleviates IDD in vitro and in vivo by activating the Nrf2/HO-1/GPX4 pathway to inhibit ferroptosis in NPCs. This mechanism suggests Td is a promising candidate for IDD treatment.

Keywords: intervertebral disc degeneration, tomatidine, Nrf 2, GPX4, ferroptosis

Introduction

With the aging of the world population, intervertebral disc degeneration (IDD) has been recognized as one of the most important causes of lower back pain.[1] However, the exact causes and mechanisms by which IDD occurs remain unclear. Under normal conditions, the anabolic and catabolic metabolism of the intervertebral disc (IVD) extracellular matrix (ECM) is in balance.[2] However, during intervertebral disc degeneration, an unfavorable IVD microenvironment leads to diminished anabolism and enhanced catabolism of the ECM.[3] There is growing evidence that one strategy for the treatment of IDD is to promote the synthesis of intervertebral disc ECM and inhibit its breakdown.[4]

In the intervertebral disc, nucleus pulposus cells (NPCs) are the primary cell type in the nucleus pulposus and are responsible for the synthesis and catabolism of ECM. Therefore, destruction of NPCs is closely related to the dysregulation of ECM synthesis and catabolism.[5] During intervertebral disc degeneration, NPCs secrete substantial amounts of pro-inflammatory factors, initiating a cascade of pathological responses. These responses lead to nucleus pulposus cell senescence and programmed cell death, resulting in decreased synthesis of aggrecan and collagen II (Col II), while simultaneously increasing the expression of matrix metalloproteinases (MMPs).[6] In recent years, a novel form

Received: 27 August 2024
Accepted: 19 December 2024
Published: 27 December 2024

of cell death known as ferroptosis has been discovered. Numerous studies have demonstrated that ferroptosis plays a key role in IDD.[7] Ferroptosis is characterized by the accumulation of iron-dependent lipid peroxides to toxic levels.[8] Senescent NPCs at the site of the medullary protrusion generate excessive reactive oxygen species (ROS), which leads to intracellular iron accumulation, depletion of glutathione (GSH), inactivation of glutathione peroxidase 4 (GPX4), and an increase in lipid peroxidation. This process disrupts iron homeostasis within the intervertebral disc and initiates ferroptosis.[9–13]

Ferroptosis is modulated by a variety of signaling pathways, among which the Nrf2/HO-1 signaling pathway plays a pivotal regulatory role in iron-induced cell death.[14–16] The nuclear factor E2-related factor 2 (Nrf2) is an antioxidant factor[17] that plays an important role in regulating the expression of antioxidant proteins and is activated in response to ROS in order to protect cells from toxic substances such as ROS.[18] During oxidative stress, Nrf2 ectopically translocates to the nucleus to activate the transcription of antioxidant enzymes, including superoxide dismutase (SOD), glutathione peroxidase (GSH-Px), and most importantly, heme oxygenase-1 (HO-1).[18,19] HO-1 has the capacity to degrade heme, resulting in the release of biliverdin, carbon monoxide, and ferrous ions.[20] The upregulation of HO-1 and its byproducts can mitigate oxidative stress damage and modulate ferroptosis.[21]

Tomatidine (Td), a natural product enriched in unripe tomatoes, has a variety of biological activities, including anti-tumor, hypolipidemic, and anti-inflammatory effects.[22] Td has been shown to inhibit age-related skeletal muscle atrophy by modulating Nrf2 and exhibiting anti-aging effects in mice.[23] In addition, Td can alleviate interleukin-1β-induced osteoarthritis and has potential therapeutic effects on osteoporosis. Meanwhile, the therapeutic effect of Td has been proven in a variety of diseases such as pancreatic cancer, hyperlipidemia, and atherosclerosis.[24–26] However, there remains a paucity of research on Td in the context of disc degeneration. In this study, we investigated the protective effects of Td on NPCs and its potential to exert antioxidant activity through the Nrf2/HO-1/GPX4 pathway, thereby alleviating LPS-induced ROS accumulation and ferroptosis. Additionally, we used a lumbar instability-induced intervertebral disc degeneration model to assess the therapeutic potential of Td for IDD. Our research further enhances the understanding of the molecular mechanisms involved in the progression of IDD, suggesting that Td holds promising potential as a therapeutic agent for IDD.

Materials and Methods

Drugs and Reagents

Tomatidine (Td, purity ≥98%) and lipopolysaccharide (LPS, purity >99%) were purchased from MCE (China). MMP3 and HO-1 antibodies were obtained from Abcam (USA; cat. nos. ab52915 and ab305290). Aggrecan neo polyclonal antibody was purchased from Thermo Fisher Scientific (UK; cat. no. PA1-1746). The collagen II antibody, ADAMTS-4 antibody, SLC40A1 antibody, xCT antibody, Nrf2 antibody, GPX4 antibody, and GAPDH antibody were from Hangzhou HuaAn Biotechnology Co., Ltd. (China; cat. nos. ER1906-48, ER1903-31, ER1916-80, HA600098, ER1706-41, ET1706-45, and ET1601-4). Ferritin light chain antibody was purchased from ABclonal (China; cat. no. A1768). Transferrin receptor antibody was purchased from Affinity (China; cat. no. AF5343). The secondary antibodies goat anti-rabbit, Alexa Fluor 488, and Alexa Fluor 594 were purchased from Hangzhou HuaAn Biotechnology Co., Ltd. (cat. nos. HA1001, HA1121, and HA1122).

Molecular Docking

Molecular docking was performed to simulate the binding of Td with Nrf2. Simulations were conducted using AutoDock Vina (Vina, version 1.1.2) with an accuracy of up to 78%. The structures of Nrf2 protein (PDB ID: 2FLU) and Td were downloaded from the RCSB and PubChem databases, respectively. For docking, the small molecule was designated as the ligand and the Nrf2 protein as the receptor. PyMOL (version 4.3.0, https://pymol.org/) was used for the isolation of the original ligands and protein structures and the removal of water and organic matter. AutoDockTools (http://mgltools.scripps.edu/downloads) was used to add hydrogen atoms, examine charges, assign atom types to AD4, and construct the docking grid box. In addition, AutoDockTools was used to determine the root of the Td ligand. Finally, the protein and small molecule structures were converted to.PDBQT format using AutoDockTools. After docking using Vina, the scores

of Nrf2 protein combined with small molecule Td were calculated. The force analysis and visualization of 3D and 2D complexes were performed using PyMOL and Discovery Studio software.

Cell Viability Assay

The viability of Td-treated NPCs was examined using a CCK-8 cell proliferation/cytotoxicity assay kit. NPCs were inoculated in 96-well plates at a density of 2×10^3 cells per well. After incubation for 24 h, the cells were treated with serial dilutions of Td (1–256 μM) for either 24 or 48 h. At the specified time points, the supernatant was carefully aspirated from each well and subsequently replaced with 100 μL of Dulbecco's Modified Eagle Medium (DMEM) containing CCK-8, according to the kit instructions. The samples were then incubated at 37°C for a duration of 90 min. Finally, the absorbance was measured using a Multiskan FC microplate luminometer (Thermo Fisher Scientific, USA).

NP Cell Culture

Rat NPCs used in this experiment were donated by Professor Di Chen (Rush University, USA). TNPCs were cultured in DMEM supplemented with 5% fetal bovine serum and 1% penicillin–streptomycin. Cells were cultured in a constant temperature incubator maintained at 5% CO_2 and 37°C. The culture media were replaced every other day. Once the cells reached approximately 90% confluence, they were harvested for experiments. NPCs were treated with either 0 or 100 ng/mL of LPS, in combination with 0, 1, 2 or 4 μM of Td for durations of 24 or 48 h.

High-Density Cell Culture

NPCs (10 μL, 1×10^7 cells/mL) were inoculated in 24-well plates and cultured for 6 h. After cell attachment, an appropriate concentration of Td was added, and the culture was maintained for 7 days. Finally, the cells were fixed with 4% paraformaldehyde (PFA), stained with toluidine blue, and subsequently scanned with an EPSON V600 photo scanner (Japan).

Extraction of RNA and Real-Time Polymerase Chain Reaction (RT-PCR)

Approximately 4×10^5 NPCs were inoculated in a 6-well plate and incubated for 24 h. After cell attachment, the cells were treated with complete medium containing LPS or Td for 48 h. Total cellular RNA was extracted using the RN28-EASYspin Plus Tissue/Cell RNA Rapid Extraction Kit (Aidlab Biotechnology, China), according to the manufacturer's instructions. Total RNA was subsequently reverse transcribed to cDNA using a HiFiScript cDNA Synthesis Kit (Cwbiotech, China), following the manufacturer's instructions. Relative quantitative real-time PCR analysis was performed using an ABI 7300 plus real-time PCR system (Applied Biosystems, USA) in conjunction with ChamQ Universal SYBR qPCR Master Mix (Vazyme, China). Table 1 shows the primer sequences.

Table 1 Primers'Sequences Used in the Real-Time PCR

Gene	Primer Sequences (5–3)	
ADAMTS-4	Forward	CGCTGAGTAGATTCGTGGAGAC
	Reverse	AGTTGACAGGGTTTCGGATGC
Collagen 2	Forward	TGACCTGACGCCCATTCATC
	Reverse	TTTCCTGTCTCTGCCTTGACCC
MMP3	Forward	TGAGCAGCAACCAGGAATAGG
	Reverse	TGAGCAGCAACCAGGAATAGG
Nrf2	Forward	GTGGTTTAGGGCAGAAGG
	Reverse	TCTTTCTTACTCTGCCTCTA
GPX4	Forward	CGATACGCTGAGTGTGGTTT
	Reverse	CGGCGAACTCTTTGATCTCTT
GAPDH	Forward	ACCCAGAAGACTGTGGATGG
	Reverse	ACCCAGAAGACTGTGGATGG

https://doi.org/10.2147/DDDT.S481714

GSH, MDA, and Ferrous Ion (Fe2+) Concentration Measurement

The MDA ELISA Kit, GSH ELISA Kit, and Cell Ferrous Iron (Fe^{2+}) Fluorometric Assay Kit were purchased from Elabscience Biotechnology Co., Ltd. (China; cat. nos. E-EL-0060, E-EL-0026, and E-BC-F101).

Standard wells (50 μL of standard solution), blank wells (50 μL of standard solution and sample diluent), and sample wells (50 μL of NPCs extract) were set up, and 50 μL of the prepared biotinylated antibody working solution was added. Plates were sealed and incubated at 37°C for 45 min. After washing the plates 3 times, 100 μL of HRP enzyme conjugate working solution was added. Plates were sealed and incubated at 37°C for 30 min. After 5 additional washes, 90 μL of substrate solution (TMB) was added, and the plates were incubated in the dark at 37°C for 15 min. Next, 50 μL of stop solution was added to terminate the reaction. The absorbance of each well at a wavelength of 450 nm was measured using a Multiskan FC microplate luminometer. MDA and GSH concentrations were calculated by constructing a standard curve.

NPCs were collected and washed twice with the reagent kit buffer. For every 1×10^6 cells, 4 μmol/L of probe was added, and the cells were incubated at 37°C in the dark for 30–60 min. Cells were centrifuged at 300×g for 5 min, the supernatant was discarded, and cells were washed again twice. After resuspending the cells in 0.2 mL of reagent kit buffer, the absorbance was measured at 542 nm using a Varioskan LUX microplate reader. The Fe^{2+} concentration was calculated by constructing a standard curve.

Western Blotting

NPCs were lysed using a mixture of phenylmethylsulfonyl fluoride and RIPA buffer (Cell Signaling Technology, USA). Protein concentrations were normalized using a BCA Kit (AMEKO, China). Protein samples (20 μg) were subjected to electrophoresis on 10% or 15% sodium dodecyl sulfate-polyacrylamide gels and then electrotransferred to polyvinylidene difluoride membranes (Bio-Rad, USA). Membranes were blocked at room temperature in Tris-buffered saline with Tween (TBST) containing 5% skimmed milk powder for 1 h. Membranes were washed 3 times using TBST for 5 min each time and then incubated in 1:1000 diluted specific primary antibody for 12 h at 4 °C with shaking. Membranes were washed 3 times using TBST for 5 min each time, incubated in the appropriate HRP-conjugated secondary antibody for 1 h at room temperature with shaking, and then again washed 3 times with TBST for 5 min each time. After cutting the membrane horizontally according to the position of the target protein, protein-antibody complexes were detected on an ImageQuant LAS-500 imaging system (GE Life Sciences, USA) using enhanced chemiluminescence reagents (Millipore, USA). Final quantitative analysis was performed with ImageJ software (NIH, USA).

Small Interfering RNA (siRNA) Transfection

Nrf2 siRNA was purchased from Suzhou Ribo Life Science Co., Ltd. (China; cat. no. siG150114100151-1-5). The transfection complex was prepared and added dropwise into NPCs containing an appropriate amount of complete culture medium without dual antibodies. The final concentration of siRNA was 50 nM. After placing the culture plates in a 37°C incubator for 24 h, an appropriate amount of LPS or Td was added to stimulate the NPCs.

Immunofluorescence Staining

NPCs were treated with LPS (100 ng/mL) and Td (2 and 4 μM) for 48 h. After fixing with 4% PFA for 15 min, the cells were permeabilized with 0.5% TritonX-100 for 30 min and washed 3 times with phosphate-buffered saline (PBS) for 5 min each time. After treatment with 1% bovine serum albumin (BSA) for 30 min, the primary antibody was diluted 1:250 and added directly without washing the cells. Cells were incubated at 4°C for 12 h and then washed 3 times with PBS for 5 min each time. After incubation with fluorescently labeled secondary antibody for 30 min at room temperature under light-proof conditions, the cells were stained with 4′,6-diamidino-2-phenylindole for 10 min. Cells were observed and photographed using a laser confocal microscope.

Flow Cytometry

The Reactive Oxygen Species (ROS) Fluorometric Assay Kit (Red) was purchased from Elabscience Biotechnology Co., Ltd. (China; cat. no. E-BC-F005). NPCs were collected, the probe was loaded according to the manufacturer's instructions, and then the ROS level in the cells was detected by flow cytometry.

In vivo Animal Experiment

Twelve-week-old C57BL/6 male mice (Shanghai Slack Laboratory Animal Co.) were randomly grouped (n = 6): sham-operated group, intervertebral disc instability (IDD) group, IDD + Td 5 mg/kg group, and IDD + Td 10 mg/kg group. For the IDD group, the supraspinous and interspinous ligaments of the lumbar spine (L3–5) were removed, and the inferior articular processes on both sides of the vertebral body were occluded to cause intervertebral instability. Mice were injected intraperitoneally with equal amounts of the indicated concentrations of Td or PBS on a fixed weekly basis and euthanized after 8 weeks. The dissected discs were fixed in 4% PFA and embedded in paraffin.

Histology and Immunohistochemistry

Samples were fixed in 10% EDTA for 14 days for decalcification, embedded in paraffin, and sections were stained with hematoxylin and eosin or Safranin O/Fast green.

For immunohistochemical staining, the sections were dewaxed, desiccated, and incubated with 3% H_2O_2 for 5 min at room temperature. The sections were blocked with PBS containing 1% goat serum albumin for 5 min. The serum was removed, and the specific primary antibody was added dropwise. Sections were incubated at 4°C for 12 h and then washed with PBS 3 times for 5 min each time. Sections were incubated with the appropriate HRP-conjugated secondary antibody for 1 h at room temperature and again washed 3 times with PBS for 5 min each time. Finally, the sections were stained with hematoxylin.

Statistical Analysis

Each value was obtained by performing at least three experiments and is represented as mean ± standard deviation (SD). Each set of values was analyzed with GraphPad Prism (USA). P-value < 0.05 indicates statistical significance.

Results

Effects of Td on NPC Viability and Proliferation

The structure of Td is shown in Figure 1A and B. To assess the effects of Td on NPC viability and proliferation, we performed a CCK-8 assay with serial dilutions of Td for 24 or 48 h. The results indicated that NPCs treated with Td at concentrations below 128 μM for 24 h did not exhibit cytotoxicity. After treating NPCs with Td for 48 h, NPCs treated with Td at concentrations below 16 μM did not show cytotoxicity. The IC50 value of Td on NPCs was 63.30 μM. Therefore, we selected concentrations of 1, 2, and 4 μM for the subsequent in vitro experiments (Figure 1C-D). We also investigated the effects of Td on LPS-treated NPCs. The results indicated that LPS treatment decreased cell proliferation. However, Td alleviated the inhibitory effect of LPS on NPC proliferation, suggesting Td exerts a protective effect on NPCs exposed to LPS (Figure 1E-F).

Td Promotes ECM Synthesis and Inhibits ECM Catabolism in NPCs in vitro

To investigate the effects of Td on ECM synthesis and degradation, we stained high-density cultured NPCs with toluidine blue. The results indicated that LPS significantly reduced the ECM area in NPCs, whereas treatment with Td could reverse this effect (Figure 2A-B). Subsequently, we analyzed gene expression in NPCs following Td treatment. In LPS-treated NPCs, the expression of ECM degradation-related genes ADAMTS-4 and MMP3 was significantly increased, while the expression of the ECM synthesis-related gene Col-2 was decreased. However, Td treatment inhibited the LPS-induced changes on NPCs (Figure 2C). Western blot analysis showed that Td promoted the expression of Col-2 and aggrecan while inhibiting the expression of ADAMTS-4 and MMP3. These findings are consistent with the results

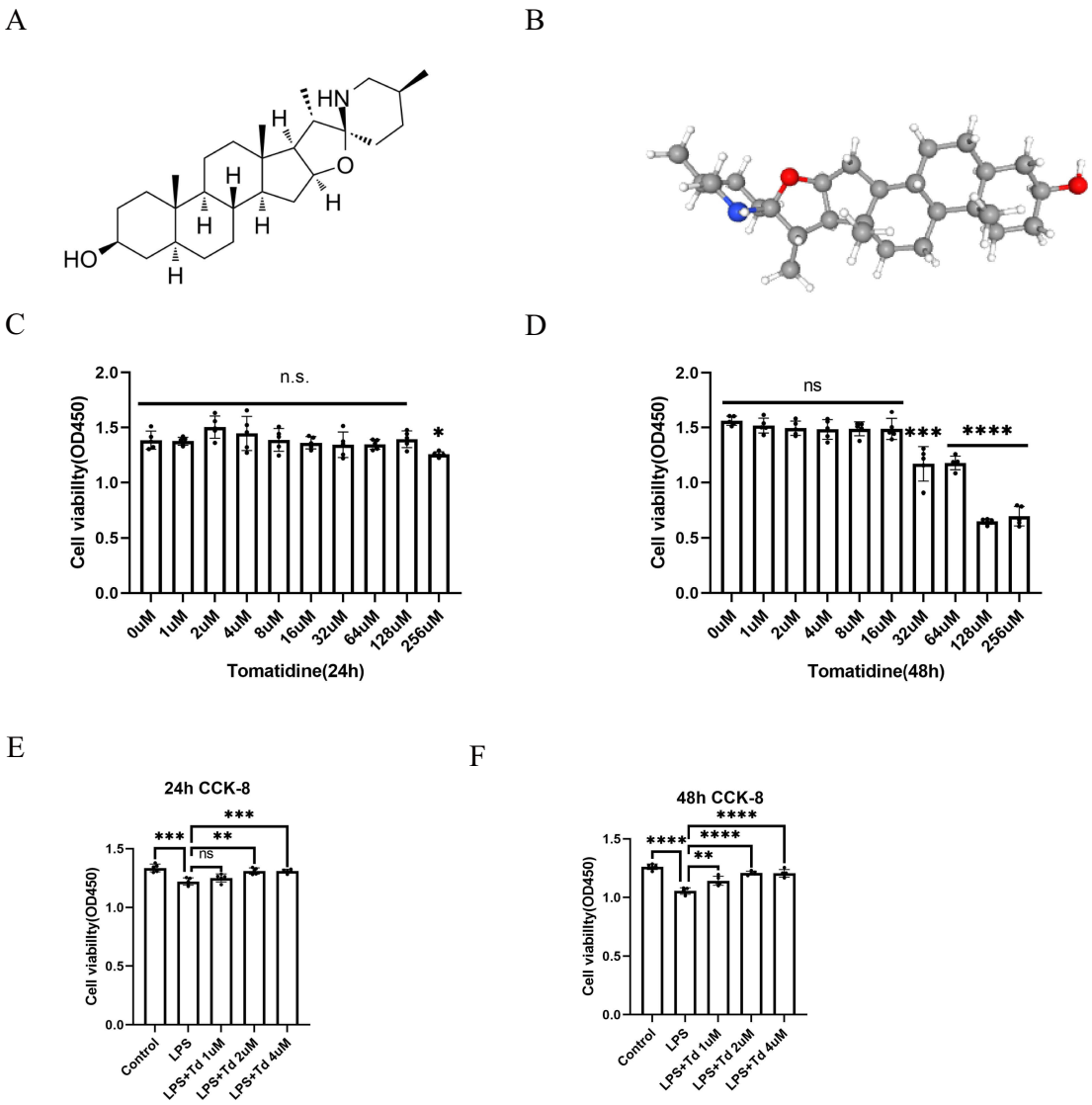

Figure 1 The effect of Td on the viability and proliferation of NPCs. (**A**) The chemical structure of Td. (**B**) The 3D structure image of Td from PubChem. (**C**) Cell counting Kit-8 assay results of NPCs stimulated with Td at different concentrations (0,1,2,4,8,16,32,64,128,256) μM at 24h. (**D**) Cell counting Kit-8 assay results of NPCs stimulated with Td at different concentrations (0,1,2,4,8,16,32,64,128,256) uM at 48h. (**E**) The results of the Cell Counting Kit-8 assay for LPS-induced NPCs after 24 hours of Td treatment. (**F**) The results of the Cell Counting Kit-8 assay for LPS-induced NPCs after 48 hours of Td treatment. All data are presented as mean ± SD. *P < 0.05, **P < 0.01, ***P < 0.001 and ****P < 0.0001, n = 5.

obtained from RT-PCR analysis (Figure 2D-E). These results indicate that Td promotes ECM synthesis and inhibits ECM degradation in NPCs, thereby contributing to the stability of the ECM.

Td Attenuates Oxidative Stress and Ferroptosis in NPCs

During IDD, oxidative stress emerges as a major driving force, contributing to ferroptosis, matrix metabolism imbalance, and inflammatory responses.[27] Oxidative stress increases the production of ROS, disrupting the intracellular antioxidant system and triggering lipid peroxidation. In addition, ROS influence iron metabolism by increasing free iron levels, with excess iron further exacerbating ROS generation while depleting glutathione (GSH) and inhibiting GPX4 activity.[28] These events directly undermine the antioxidant defense system and diminish the cellular resistance to ferroptosis, rendering cells more susceptible to ferroptosis and intensifying oxidative damage within the IVD. In this experiment, we measured the levels of ROS in NPCs. The results indicated a significant increase in ROS levels following LPS treatment, whereas ROS levels were significantly inhibited after Td treatment (Figure 3A). Malondialdehyde (MDA), a marker of

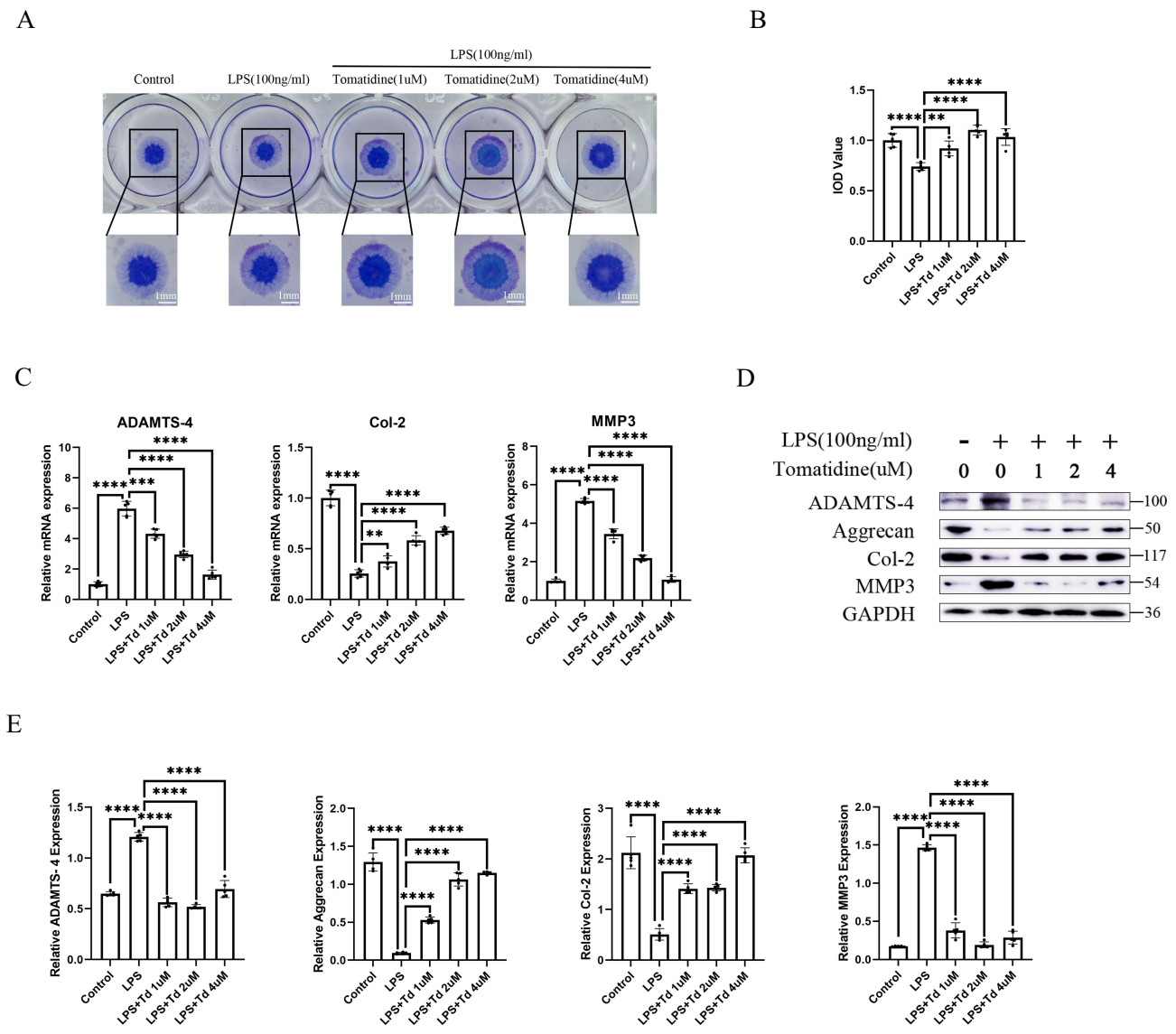

Figure 2 The effect of Td on ECM synthesis and catabolism of NPCs in vitro.(**A**) Toluidine blue staining for the high-density culture of NPCs for 1 week (scale bar: 1mm). (**B**) The integrated optical density (IOD) value of NPCs was analyzed using Image J. (**C**) The gene expression ADAMTS-4, Col-2 and MMP3 were detected by qPCR in the NPCs, treated with or without the administration of LPS for 24h. (**D** and **E**)Western blot analysis of ADAMTS-4, Aggrecan, Col-2, MMP3 and GAPDH expression in NPCs stimulated with LPS (100 ng/mL). The protein expression were evaluated by Image J. All data are presented as mean ± SD. **P < 0.01, ***P < 0.001 and ****P < 0.0001, n = 5.

the oxidative degradation of polyunsaturated fatty acids under the attack of ROS, was elevated in response to LPS, indicating an increase in oxidative stress. Glutathione (GSH), a key intracellular antioxidant, scavenges ROS and maintains redox balance within cells. Therefore, we assessed the levels of MDA and GSH in the cells. The results indicated that LPS treatment increased MDA levels and decreased GSH levels in NPCs. However, following Td treatment, the effects of LPS on MDA and GSH levels were reversed (Figure 3B), suggesting Td can alleviate the oxidative stress induced by LPS in NPCs. Subsequently, we observed an increase in the concentration of ferrous ions in NPCs following LPS treatment, indicating that LPS activates ferroptosis in NPCs. However, after Td treatment, the concentration of ferrous ions in NPCs decreased, demonstrating Td can inhibit LPS-induced ferroptosis in NPCs (Figure 3C). Western blot analysis indicated that after LPS treatment, the expression of TFR within the ferroptosis-related pathway was increased, while the expression of xCT, SLC40A1, and FTL was decreased. However, this phenomenon is reversed after Td treatment (Figure 3D-E). The expression of TFR, as assessed by confocal microscopy,

https://doi.org/10.2147/DDDT.S481714

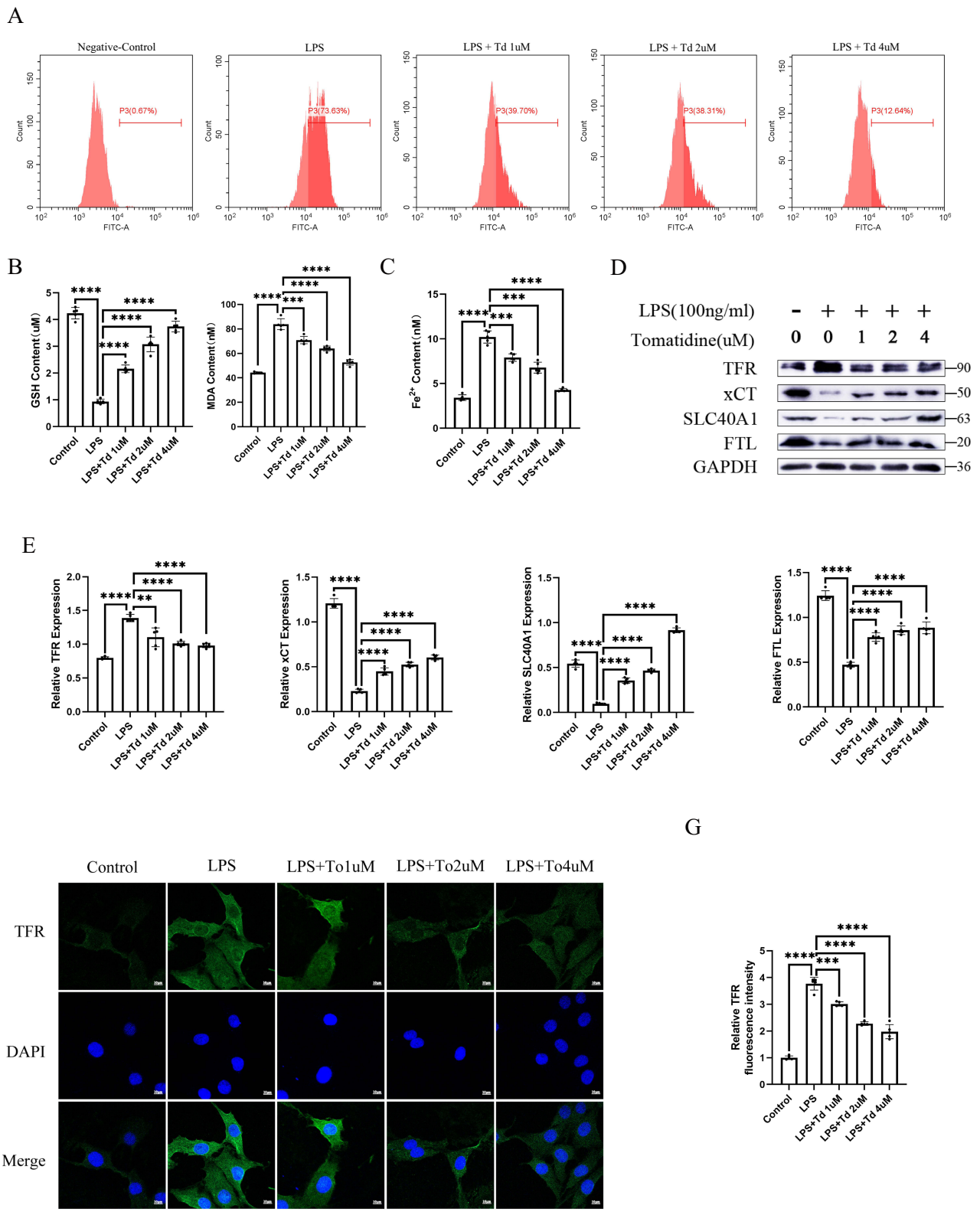

Figure 3 Protective effect of Td against oxidative stress and ferroptosis in NPCs. (**A**) The intracellular ROS levels in NPCs were measured by flow cytometry assay. (**B**)The levels of GSH and MDA in NPCs were determined by ELISA. (**C**) The content of ferrous iron (Fe2+) within cells was assessed using the Cell Ferrous Iron (Fe2+) Fluorometric Assay Kit. (**D** and **E**) Western blot analysis of TFR, xCT, SLC40A1, FTL and GAPDH expression in NPCs stimulated with LPS (100 ng/mL). The protein expression were evaluated by Image J. (**F** and **G**) The protein expression of TFR was evaluated by cell immunofluorescence (scale bar: 10 μm) and Image J. All data are presented as mean ± SD. **P < 0.01, ***P < 0.001 and ****P < 0.0001, n = 5.

https://doi.org/10.2147/DDDT.S481714

was consistent with the Western blot results (Figure 3F-G), suggesting Td may exert a protective effect by inhibiting oxidative stress and ferroptosis in NPCs.

Td Exerts a Protective Role in NPCs Through the Nrf2/HO-1/GPX4 Axis

The Nrf2/HO-1/GPX4 pathway plays a crucial role in antioxidant defense and stress response, regulating ferroptosis by influencing oxidative stress, iron metabolism, and lipid peroxidation.[29] We conducted two-dimensional and three-dimensional force analysis and visualization of Td and Nrf2 through molecular docking simulations (Figure 4A-B). The results showed that the small molecule ligand Td bound to Nrf2 through two hydrogen bonds (3.7 and 4.0 Å) with arginine residues 367 and 415 of the receptor protein, respectively, and two hydrophobic interactions (3.3 and 3.8 Å) with valine residues 418 and 606, respectively. The binding energy of Td to Nrf2 was −11.9 kcal/mol. Subsequently, RT-PCR results indicated that Nrf2 expression was reduced in NPCs treated with LPS. However, Td treatment increased Nrf2 expression, which was accompanied by an increase in GPX4 expression (Figure 4C). Similar results were observed in Western blot and cellular immunofluorescence experiments, indicating Td can enhance the expression of Nrf2, as well as promote the expression of HO-1 and GPX4 (Figure 4D-G). These findings suggest that Td exerts its antioxidant and antiferroptosis effects through the Nrf2/HO-1/GPX4 axis.

Silencing of Nrf2 Markedly Reduced the Influence of Td on ECM Metabolism in NPCs

To further confirm that Td exerts its protective effect on NPCs through Nrf2, we used Nrf2 siRNA to suppress its expression. Cells were divided into control, LPS stimulated, LPS + Td 4 μM, siRNA, and LPS + Td 4 μM + siRNA groups and treated for 72 h. We verified that siRNA knocked down the expression of Nrf2 by RT-PCR (Figure 5A). Western blot results indicated that LPS treatment increased the expression of ECM synthesis-related proteins Col-2 and aggrecan while inhibiting the expression of ECM degradation-related proteins ADAMTS-4 and MMP3. The effects of Td in NPCs were significantly abolished following the downregulation of Nrf2 expression (Figure 5B-C). Cellular immunofluorescence experiments revealed that the effect of Td in promoting Col-2 expression was significantly inhibited under conditions of reduced Nrf2 expression (Figure 5D-E), indicating Td exerts its protective effects in NPCs in a manner dependent on the presence of Nrf2.

Silencing of Nrf2 Significantly Reduces the Ability of Td to Inhibit Oxidative Stress and Ferroptosis

Nrf2 is a key transcription factor that regulates oxidative stress and ferroptosis.[30] We measured the levels of ROS in NPCs after the knockdown of Nrf2. The results revealed that Td was no longer able to reduce the elevated ROS levels induced by LPS, leading to sustained oxidative stress in NPCs (Figure 6A). Western blot analysis indicated that Td inhibited the LPS-induced upregulation of TFR and SLC40A1 protein expression, while also significantly suppressing the LPS-induced downregulation of GPX4 and FTL protein expression. However, the effect of Td on NPCs was abolished after the knockdown of Nrf2 (Figure 6B-C). Confocal microscopy experiments further confirmed these results, indicating Nrf2 siRNA reversed the effect of Td on TFR expression in NPCs (Figure 6D-E). These results confirm that Td inhibits oxidative stress and ferroptosis through the Nrf2/HO-1/GPX4 axis.

Tomatidine Alleviates Intervertebral Disc Degeneration in Mice

The effect of Td in vivo was verified by histological examination. Hematoxylin and eosin staining and Sirius Red-O (S-O) staining confirmed that the degenerated IVD was characterized by NP fissures, inwardly projecting annulus fibrosus (AF), and hypertrophic AF cells. After Td treatment, the number of NPCs increased, and their distribution became more uniform. The proteoglycan staining exhibited a darker coloration, indicating an increase in matrix content. Collagen fibers were arranged more densely, with fewer instances of fiber rupture or repair. The thickness of the cartilage endplate increased, and fissures were reduced or repaired. We performed histological scoring of the discs in each group,[31] which showed that the degree of degeneration decreased as the concentration of Td was increased (Figure 7A-B). These findings suggest that the histological characteristics of the IVD in treated mice demonstrate alleviated degeneration, with

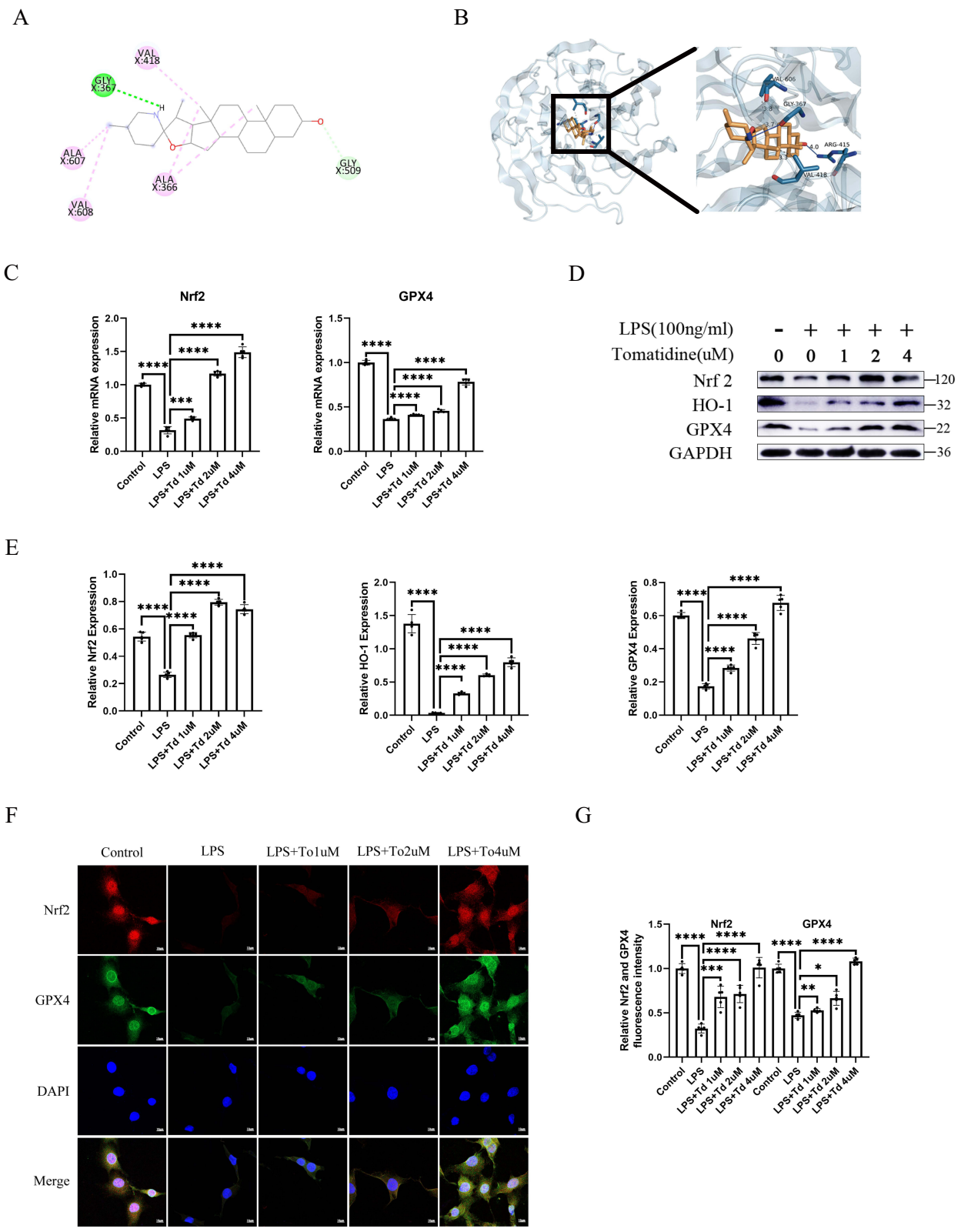

Figure 4 Td can target the Nrf2/HO-1/GPX4 axis for potential effects. (**A**)Results of Td force analysis of 2D images. (**B**) The 3D structure image of Td interacting with Nrf2 in the image. (**C**) The gene expression Nrf2 and GPX4 were detected by qPCR in the NPCs, treated with or without the administration of LPS for 24h. (**D** and **E**) Western blot analysis of Nrf2, HO-1, GPX4 and GAPDH expression in NPCs stimulated with LPS (100 ng/mL). The protein expression were evaluated by Image J. (**F** and **G**) The protein expression of Nrf2 and GPX4 was evaluated by cell immunofluorescence (scale bar: 10 μm) and Image J. All data are presented as mean ± SD. *P < 0.05, **P < 0.01, ***P < 0.001 and ****P < 0.0001, n = 5.

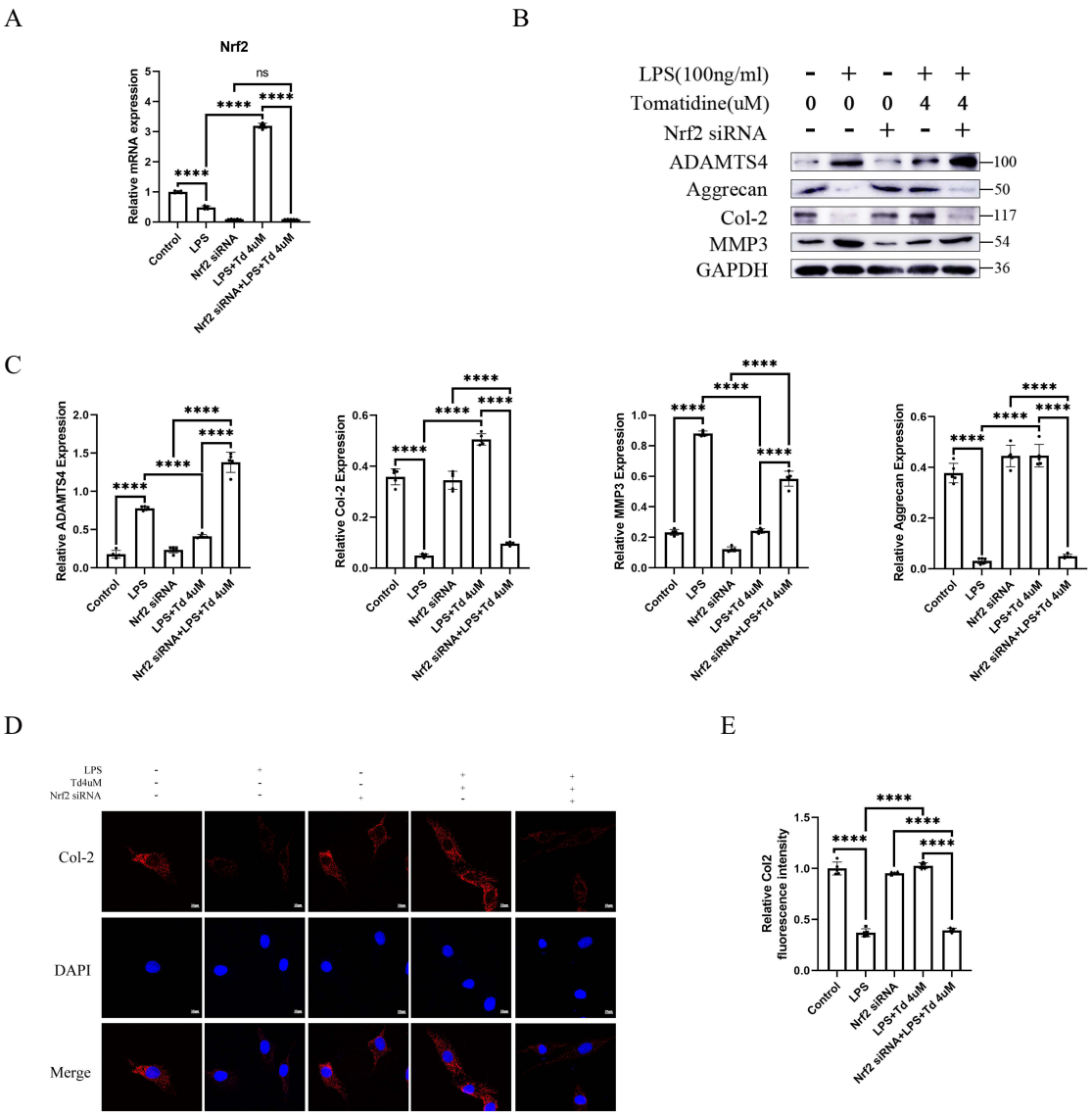

Figure 5 The protective effect of Td on NPCs was reversed after Nrf2 was silenced. (**A**) The gene expression Nrf2 was detected by qPCR in the NPCs, treated with or without the administration of LPS for 24h. (**B** and **C**) After Nrf2 was silenced, Western blot analysis of ADAMTS-4, Aggrecan, Col-2, MMP3 and GAPDH expression in NPCs. Protein expression was assessed by Image J. (**D** and **E**) Col-2 expression was assessed by cellular immunofluorescence (scale bar: 10 μm) and Image J after Nrf2 was silenced. All data are presented as mean ± SD. ****P < 0.0001, n = 5.

overall structure and function approaching normalcy. We then performed immunohistochemical staining, which showed that the expression of the ECM catabolic marker MMP3 was significantly higher and that of the ECM anabolic marker Col-2 was significantly lower in the IDD surgery group relative to the control sham surgery group (Figure 7C-F). At the same time, we observed a significant decrease in the expression of Nrf2 and GPX4 in the IVD of the IDD surgery group compared to the sham surgery group (Figure 7G-H). However, Td treatment promoted the expression of Col-2, Nrf2, and GPX4 in the IVD while inhibiting the expression of MMP3. These results indicate that under Td treatment, the Nrf2/HO-1/GPX4 axis is activated, which enhances the anabolic metabolism of the ECM in NPCs and suppresses the catabolic metabolism of the ECM within these cells. At the same time, we assessed the impact of Td on the heart, liver, and kidneys of mice using hematoxylin and eosin staining. The results indicated that Td did not exhibit any toxic effects on the vital organs of the mice (Figure S1A). The results are consistent with in vitro experiments, indicating Td exerts a protective effect on the ECM of NPCs, alleviating its degradation during the degenerative process. Td mitigates

https://doi.org/10.2147/DDDT.S481714

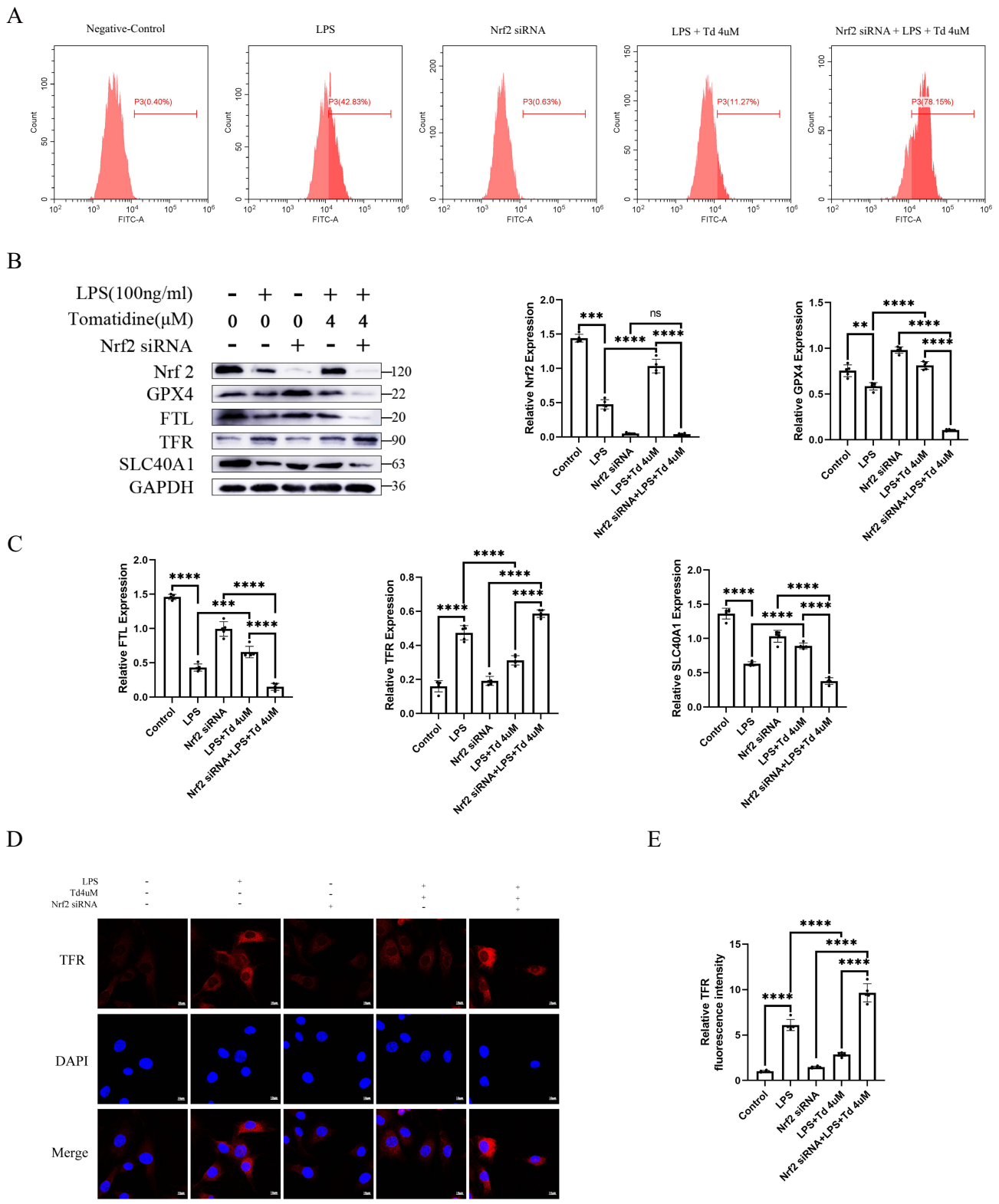

Figure 6 The inhibition of oxidative stress and ferroptosis by Td was reversed after Nrf2 was silenced. (**A**) After Nrf2 was silenced, the intracellular ROS levels in NPCs were measured by flow cytometry assay. (**B** and **C**) After Nrf2 was silenced, Western blot analysis of Nrf2, GPX4, FTL, TFR, SLC40A1 and GAPDH expression in NPCs. Protein expression was assessed by Image J. (**D** and **E**) TFR expression was assessed by cellular immunofluorescence (scale bar: 10 μm) and Image J after GPX4 was silenced. All data are presented as mean ± SD. **P < 0.01, ***P < 0.001 and ****P < 0.0001, n = 5.

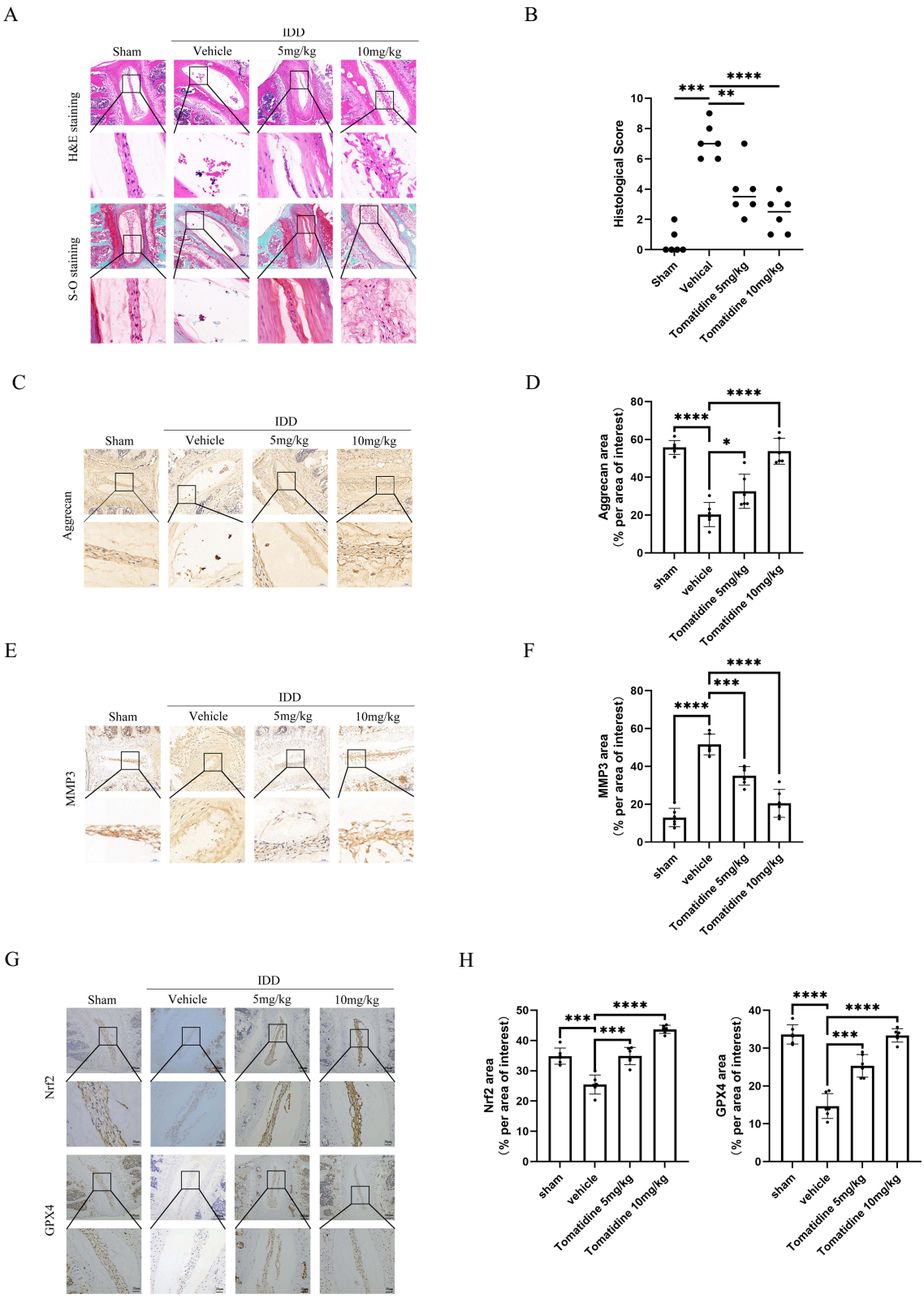

Figure 7 Amelioration of IDD in the IDD mouse model in vivo by Td. (**A**) Hematoxylin and eosin staining and Safranin O-Fast green staining were performed after 8 weeks of intraperitoneal injection (n=6, Scale bar: 100 μm/20 μm). (**B**) Histologic score of intervertebral discs in each group. (**C** and **D**) Immunohistochemical images of Aggrecan of intervertebral disc (n=6, Scale bar: 100 μm/20 μm), average percentage of positive staining area of intervertebral disc was assessed by Image J. (**E** and **F**) Immunohistochemical images of MMP3 of intervertebral disc (n=6, Scale bar: 100 μm/20 μm), average percentage of positive staining area of intervertebral disc was assessed by Image J. (**G** and **H**) Immunohistochemical images of Nrf2 and GPX4 in intervertebral disc tissues (n=6, Scale bar: 100 μm/20 μm), average percentage of positive staining area of intervertebral disc was assessed by Image J.All data are presented as mean ± SD. *P < 0.05, **P < 0.01, ***P < 0.001 and ****P < 0.0001.

https://doi.org/10.2147/DDDT.S481714

ferroptosis in NPCs and delays IDD induced by lumbar spine instability through the activation of the Nrf2/HO-1/GPX4 axis.

Discussion

IDD is the leading cause of chronic lower back pain and a significant contributor to disability in adults.[32] This study aims to identify a novel therapeutic agent to halt the progression of IDD. We investigated the therapeutic effects of Td on IDD and demonstrated its efficacy in vitro and in vivo. In vitro experiments revealed that Td promotes the synthesis of the ECM while reducing its degradation. This effect is mediated through the Nrf2/HO-1/GPX4 signaling pathway, which effectively mitigates ROS and inhibits ferroptosis. Furthermore, Td significantly improved IDD in a murine model of lumbar instability.

Previous studies have indicated the crucial role of the ECM in the nucleus pulposus in maintaining IVD stability, emphasizing its relevance in IDD pathophysiology and treatment strategies.[33–35] Lipopolysaccharide, a well-established stimulant, induces degeneration of NPCs.[36] Therefore, we used LPS to establish an in vitro IDD model. Our findings revealed that LPS stimulation significantly decreased the expression of ECM synthesis-related proteins, such as Col-2 and aggrecan while increasing the expression of ECM degradation-related proteins such as MMP3 and ADAMTS-4. However, treatment with Td countered the inhibitory effects of LPS on NPCs. High-density cultured NPCs treated with Td showed results that were consistent with those obtained from Western blotting and RT-PCR analyses, and compared to the LPS-treated group, these cells exhibited enhanced ECM synthesis.

Td mitigates oxidative stress and ferroptosis in NPCs during the progression of IDD, potentially through the activation of the Nrf2/HO-1/GPX4 signaling pathway. The Nrf2 signaling pathway is recognized as a key antioxidant mechanism.[37] In this study, we elucidated the interaction between Td and Nrf2 through molecular docking, providing a theoretical basis for targeting Nrf2 with Td. Flow cytometry analysis demonstrated that Td treatment reduced ROS and ferrous ion levels. Subsequent Western blot analysis revealed that Td increased the expression of ferroptosis-associated proteins such as GPX4, TFR, and SLC40A1 while decreasing TFR expression. However, silencing Nrf2 expression through siRNA reversed the effects of Td on oxidative stress and ferroptosis, resulting in a loss of its protective effect on NPCs. These findings suggest that Td mitigates oxidative stress and ferroptosis during IDD by activating the Nrf2/HO-1/GPX4 signaling pathway.

To confirm the treatment effects of Td on IDD in vivo, we used a murine model of IDD induced by resection of the supraspinous and interspinous ligaments (L3-5) combined with occlusion of the lower articular processes on both sides of the vertebrae. Histological staining results showed that Td treatment reduced fissures in the nucleus pulposus and decreased disorganization within the annulus fibrosus. Furthermore, immunohistochemical analysis revealed increased expression of aggrecan, Nrf2, and GPX4 after Td treatment, while MMP3 expression was decreased. These findings are consistent with those from in vitro experiments. Therefore, we conclude that Td can inhibit the progression of IDD in vivo, suggesting its potential as an effective therapeutic agent for treating IDD.

This study has certain limitations. Firstly, while LPS can partially simulate the progression of IDD, the actual environment within the IVD is complex, involving numerous factors that are challenging to control. The downstream genes of Nrf2 include HO-1, solute carrier family 7 member 11 (SLC7A11/xCT), GSH S-transferase, GPX4, and GSH reductase, among others.[38] A previous study has indicated that Nrf2 is a crucial regulator of ferroptosis, modulating its progression through various mechanisms.[39] In this study, we demonstrate that Td inhibits ferroptosis through the Nrf2/HO-1/GPX4 signaling pathway. However, we did not explore other signaling molecules downstream of Nrf2, and future research will aim to identify these new pathways. Finally, our study lacks a model for natural degeneration. While we have used a more widely accepted lumbar instability model, we are unable to alleviate the effects of trauma-induced inflammation. Therefore, we are considering the use of natural degeneration models in future studies to gain deeper insights into the role of Td in the treatment of IDD.

Conclusion

In summary, our study demonstrates that Td exerts protective effects on nucleus pulposus cells in vivo and in vitro. The mechanism of action of Td involves the Nrf2/HO-1/GPX4 signaling pathway, suggesting it holds promise as a safe and effective therapeutic agent for the treatment of IDD (Figure 8).

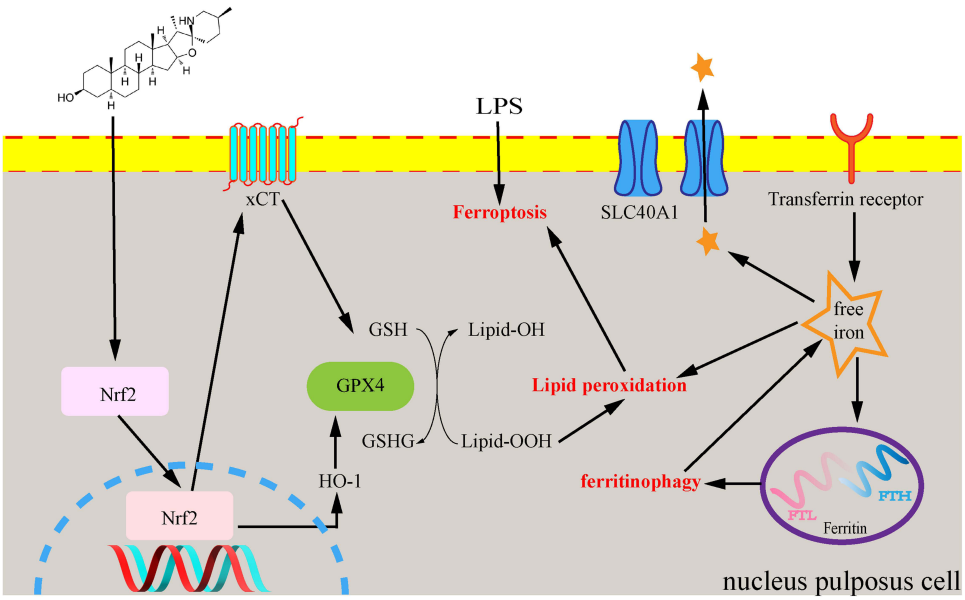

Figure 8 Schematic representation of Td inhibiting IDD. Td inhibits ferroptosis in NPCs by promoting the activation of Nrf2/HO-1/GPX4 signaling.

Abbreviations

ADAMTS-4, A disintegrin and metalloprotease with thrombospondin 4; Nrf 2, Nuclear factor erythroid2-related factor 2; COL 2, Collagen II; TFR, Transferrin receptor; FTL, Ferritin light chain; DAPI, 4′,6-Diamidino-2-phenylindole hydrochloride; MMP, Motifs matrix metalloproteinase; NPCs, Nucleus pulposus cells; Td, Tomatidine; GPX4, Glutathione peroxidase 4; IDD, Intervertebral disc degeneration; IVD, Intervertebral disc; ECM, Extracellular matrix; NPCs, Nucleus pulposus cells.

Ethics Statement

The animal study was reviewed and approved by Animal Ethics Committee of Taizhou Hospital (Approval number: TZY-2022151). All operations comply with IACUC (Institutional Animal Care and Use Committee) regulations and guidelines to ensure the welfare of laboratory animals.

Acknowledgments

Thanks to the support of the public experimental platform at Taizhou Hospital. We thank International Science Editing (http://www.internationalscienceediting.com) for editing this manuscript.

Funding

This research was partially supported by the Basic Public Welfare Research Project of Zhejiang Province (LGF19H060004), the Science and Technology Program of Traditional Chinese Medicine Science and Technology of Zhejiang Province (2018ZB138), the Science and Technology Planning Program of Taizhou City (1802KY04), and the Taizhou Social Development Science and Technology Project of Zhejiang Province (21ywa54).

Disclosure

The authors declare that they have no known competing financial interests or personal relationships that could have appeared to influence the work reported in this paper.

References

1. Knezevic NN, Candido KD, Vlaeyen JWS, Van Zundert J, Cohen SP. Low back pain. *Lancet*. 2021;398(10294):78–92. doi:10.1016/S0140-6736(21)00733-9

2. Zhang W, Gong Y, Zheng X, et al. Platelet-derived growth factor-BB inhibits intervertebral disc degeneration via suppressing pyroptosis and activating the MAPK signaling pathway. *Front Pharmacol*. 2022;12:799130. doi:10.3389/fphar.2021.799130
3. Francisco V, Pino J, González-Gay MÁ, et al. A new immunometabolic perspective of intervertebral disc degeneration. *Nat Rev Rheumatol*. 2022;18(1):47–60. doi:10.1038/s41584-021-00713-z
4. Xin J, Wang Y, Zheng Z, Wang S, Na S, Zhang S. 5, treatment of intervertebral disc degeneration. *Orthop Surg*. 2022;14(7):1271–1280. doi:10.1111/os.13254
5. Vergroesen PP, Kingma I, Emanuel KS, et al. Mechanics and biology in intervertebral disc degeneration: a vicious circle. *Osteoarthritis Cartilage*. 2015;23(7):1057–1070. doi:10.1016/j.joca.2015.03.028
6. Fan C, Chu G, Yu Z, et al. The role of ferroptosis in intervertebral disc degeneration. *Front Cell Dev Biol*. 2023;11:1219840. doi:10.3389/fcell.2023.1219840
7. Ohnishi T, Iwasaki N, Sudo H. Causes of and molecular targets for the treatment of intervertebral disc degeneration a review. *Cells*. 2022;11(3):394. doi:10.3390/cells11030394
8. Zhang S, Sun Z, Jiang X, et al. Ferroptosis increases obesity: crosstalk between adipocytes and the neuroimmune system. *Front Immunol*. 2022;13:1049936. doi:10.3389/fimmu.2022.1049936
9. Zhang Y, Huang X, Qi B, et al. Ferroptosis and musculoskeletal diseases: "Iron Maiden" cell death may be a promising therapeutic target. *Front Immunol*. 2022;13:972753. doi:10.3389/fimmu.2022.972753
10. Zheng J, Conrad M. The Metabolic Underpinnings of Ferroptosis. *Cell Metab.* 2020;32(6):920–937. doi:10.1016/j.cmet.2020.10.011
11. Jiang X, Stockwell BR, Conrad M. Ferroptosis: mechanisms, biology and role in disease. *Nat Rev Mol Cell Biol*. 2021;22(4):266–282. doi:10.1038/s41580-020-00324-8
12. Zhuang Y, Liu L, Liu M, et al. The sonic hedgehog pathway suppresses oxidative stress and senescence in nucleus pulposus cells to alleviate intervertebral disc degeneration via GPX4. *Biochim Biophys Acta Mol Basis Dis*. 2024;1870(2):166961. doi:10.1016/j.bbadis.2023.166961
13. Gao X, Hu W, Qian D, et al. The mechanisms of ferroptosis under hypoxia. *Cell Mol Neurobiol*. 2023;43(7):3329–3341. doi:10.1007/s10571-023-01388-8
14. Dang R, Wang M, Li X, et al. Edaravone ameliorates depressive and anxiety-like behaviors via Sirt1/Nrf2/HO-1/Gpx4 pathway. *J Neuroinflammation*. 2022;19(1):41. doi:10.1186/s12974-022-02400-6
15. Deng HF, Yue LX, Wang NN, et al. Mitochondrial iron overload-mediated inhibition of Nrf2-HO-1/GPX4 assisted ALI-Induced Nephrotoxicity. *Front Pharmacol*. 2020;11:624529. doi:10.3389/fphar.2020.624529
16. Niu C, Jiang D, Guo Y, et al. Spermidine suppresses oxidative stress and ferroptosis by Nrf2/HO-1/GPX4 and Akt/FHC/ACSL4 pathway to alleviate ovarian damage. *Life Sci*. 2023;332:122109. doi:10.1016/j.lfs.2023.122109
17. Chen Y, Zhu S, Chen Z, et al. Gingerenone A alleviates ferroptosis in secondary liver injury in colitis mice via activating Nrf2-Gpx4 signaling pathway. *J Agric Food Chem*. 2022;70(39):12525–12534. doi:10.1021/acs.jafc.2c05262
18. Abdulaal WH, Omar UM, Zeyadi M, et al. Modulation of the crosstalk between Keap1/Nrf2/HO-1 and NF-κB signaling pathways by Tomatidine protects against inflammation/oxidative stress-driven fulminant hepatic failure in mice. *Int Immunopharmacol*. 2024;130:111732. doi:10.1016/j.intimp.2024.111732
19. Yang S, Kuang G, Zhang L, et al. Mangiferin Attenuates LPS/D-GalN-induced acute liver injury by promoting HO-1 in Kupffer Cells. *Front Immunol*. 2020;11:285. doi:10.3389/fimmu.2020.00285
20. Consonni FM, Incerti M, Bertolotti M, Ballerini G, Garlatti V, Sica A. Heme catabolism and heme oxygenase-1-expressing myeloid cells in pathophysiology. *Front Immunol*. 2024;15:1433113. doi:10.3389/fimmu.2024.1433113
21. Li N, Hao L, Li S, et al. The NRF-2/HO-1 signaling pathway: a promising therapeutic target for metabolic dysfunction-associated steatotic liver disease. *J Inflamm Res*. 2024;17:8061–8083. doi:10.2147/JIR.S490418
22. Wu S-J, Huang W-C, Yu M-C, et al. Tomatidine ameliorates obesity-induced nonalcoholic fatty liver disease in mice. *J Nutr Biochem*. 2021;91:108602. doi:10.1016/j.jnutbio.2021.108602
23. Fang EF, Waltz TB, Kassahun H, et al. Tomatidine enhances lifespan and healthspan in C. elegans through mitophagy induction via the SKN-1/Nrf2 pathway. *Sci Rep*. 2017;7(1):46208. doi:10.1038/srep46208
24. Chu X, Yu T, Huang X, et al. Tomatidine suppresses inflammation in primary articular chondrocytes and attenuates cartilage degradation in osteoarthritic rats. *Aging*. 2020;12(13):12799–12811. doi:10.18632/aging.103222
25. Fujiwara Y, Kiyota N, Tsurushima K, et al. Tomatidine, a tomato sapogenol, ameliorates hyperlipidemia and atherosclerosis in ApoE-deficient mice by inhibiting Acyl-CoA:cholesterol Acyl-transferase (ACAT. *Journal of Agricultural and Food Chemistry*. 2012;60(10):2472–2479. doi:10.1021/jf204197r
26. Yu T, Wu Q, You X, et al. Tomatidine alleviates osteoporosis by downregulation of p53. *Med Sci Monit*. 2020;26. doi:10.12659/MSM.923996
27. Wang W, Jing X, Du T, et al. Iron overload promotes intervertebral disc degeneration via inducing oxidative stress and ferroptosis in endplate chondrocytes. *Free Radic Biol Med*. 2022;190:234–246. doi:10.1016/j.freeradbiomed.2022.08.018
28. Li F, Li S, Shi Y, et al. Glutathione: a key regulator of extracellular matrix and cell death in intervertebral disc degeneration. *Mediators Inflamm 2024*. 2024;2024(1):4482642. doi:10.1155/2024/4482642
29. Zhang CY, Hu XC, Zhang GZ, Liu MQ, Chen HW, Kang XW. Role of Nrf2 and HO-1 in intervertebral disc degeneration. *Connect Tissue Res*. 2022;63(6):559–576. doi:10.1080/03008207.2022.2089565
30. Chen Y, Jiang Z, Li X. New insights into crosstalk between Nrf2 pathway and ferroptosis in lung disease. *Cell Death Dis*. 2024;15(11):841. doi:10.1038/s41419-024-07224-1
31. Tam V, Chan WCW, Leung VYL, et al. Histological and reference system for the analysis of mouse intervertebral disc: HISTOLOGICAL GRADING OF MOUSE DISC. *J Orthop Res*. 2017; 36(1):233–243.
32. Zhao D, Dou YX, Zeng LF, et al. The effects of extracellular matrix-degrading enzymes polymorphisms on intervertebral disc degeneration. *JOR Spine*. 2024;7(4):e70012. doi:10.1002/jsp2.70012
33. Cazzanelli P, Wuertz-Kozak K. MicroRNAs in intervertebral disc degeneration, apoptosis, inflammation, and mechanobiology. *Int J Mol Sci*. 2020;21(10):3601. doi:10.3390/ijms21103601
34. Krut Z, Pelled G, Gazit D, Gazit Z. Stem cells and exosomes: new therapies for intervertebral disc degeneration. *Cells*. 2021;10(9):2241. doi:10.3390/cells10092241

35. Mohd Isa IL, Teoh SL, Mohd Nor NH, Mokhtar SA. Discogenic low back pain: anatomy, pathophysiology and treatments of intervertebral disc degeneration. *Int J Mol Sci*. 2022;24(1):208. doi:10.3390/ijms24010208
36. Peng X, Ji HY, Gao JW, et al. YAP1 exacerbates pyroptosis and senescence in nucleus pulposus cells by promoting BNIP3-mediated mitophagy. *Int Immunopharmacol*. 2024;143(Pt 2):113434. doi:10.1016/j.intimp.2024.113434
37. Marchev AS, Dimitrova PA, Burns AJ, Kostov RV, Dinkova-Kostova AT, Georgiev MI. Oxidative stress and chronic inflammation in osteoarthritis: can NRF2 counteract these partners in crime?: the regulatory role of NRF2 in osteoarthritis. *Ann. N.Y. Acad. Sci.* 2017;1401(1):114–135. doi:10.1111/nyas.13407
38. Saha S, Buttari B, Panieri E, Profumo E, Saso L. An overview of Nrf2 signaling pathway and its role in inflammation. *Molecules*. 2020;25(22):5474. doi:10.3390/molecules25225474
39. Anandhan A, Dodson M, Schmidlin CJ, Liu P, Zhang DD. Breakdown of an ironclad defense system: the critical role of NRF2 in mediating ferroptosis. *Cell Chem. Biol.* 2020;27(4):436–447. doi:10.1016/j.chembiol.2020.03.011